THE
PHYSICAL REVIEW

A journal of experimental and theoretical physics established by E. L. Nichols in 1893

SECOND SERIES, Vol. 138, No. 5B 7 JUNE 1965

Decay of Pd^{100} to Odd-Odd Rh^{100}†

J. S. EVANS* AND R. A. NAUMANN
Frick Chemical Laboratory, Palmer Physical Laboratory, and Princeton-Pennsylvania Accelerator, Princeton University, Princeton, New Jersey
(Received 27 January 1965)

The gamma-ray and conversion-electron spectra accompanying the decay of 4.0-day Pd^{100} have been studied using a lithium-drifted germanium detector, permanent-magnet spectrographs, and an orange beta-ray spectrometer. Strong transitions with indicated multipolarities have been found at 32.72 ($M1+E2$), 42.10 ($E1$), 74.77 ($E1$), 84.00 ($M1$), and 126.07 ($E1$) keV; weaker transitions have been observed at 55.82, 139.72, 151.55, and 158.77 ($E1$) keV. The level scheme of odd-odd Rh^{100} has been elucidated, using conversion electron–γ-ray coincidence measurements. Levels in Rh^{100} are indicated at 0 (1−), 32.70 (2−), 74.79 (2+), 158.77 (1+), and 214.6 (+) keV. Delayed-coincidence events were observed between the strong 74.77- and 84.00-keV transitions, indicating a lifetime of 0.18 ± 0.02 μsec for the 74.79-keV level in Rh^{100}. It is suggested that two different proton configurations $(g_{9/2})^5$ and $(g_{9/2})^4p_{1/2}$ contribute to the positive- and negative-parity Rh^{100} states, respectively. Proton and neutron shell-model configurations are suggested for several levels. A jj-coupling model is used to interpret the spins and parities of the observed levels.

I. INTRODUCTION

UNTIL quite recently, very little data had been reported concerning the levels in Rh^{100} populated by the decay of 4.0-day Pd^{100}. Marquez[1] reported a single transition at 80.7 ± 0.4 keV. The chart of the nuclides lists the gamma radiations of Pd^{100} as 0.082, 0.073, and 0.04–0.31 MeV, but these data were never published.[2] In a paper on levels in Ru^{100}, Koike *et al.*[3] reported several conversion lines which they attributed to Pd^{100} decay but did not otherwise interpret.

During an investigation of Pd^{101} decay in these laboratories,[4] several conversion-electron lines, converted in rhodium and having a 4-day half-life, were observed and assigned to transitions in Rh^{100}. Since this present study began, two publications on Pd^{100} decay have appeared. Rogachev and Nikitin[5] reported conversion lines arising from three transitions at approximately 32.3, 74.4, and 83.8 keV. Anton'eva *et al.*[6] presented additional conversion lines, a gamma spectrum, and a level scheme for Rh^{100} based on gamma-gamma coincidence measurements.

The present work includes delayed-coincidence measurements of the prominent 84–75-keV cascade, showing that the 75-keV transition is greatly hindered. This fact necessitates an inversion of the level scheme proposed by Anton'eva *et al.* A detailed investigation of Pd^{100} decay was undertaken to elucidate the nature of the low-lying levels in Rh^{100}. Since only a few levels at very low energies are populated, it was hoped to understand the spins and parities of the levels in odd-odd Rh^{100} within the framework of a jj-coupling model.

II. SOURCE PREPARATION

Rhodium-foil targets were bombarded with 42-MeV protons in the Nevis Synchrocyclotron, Columbia University, producing Pd^{100} by the $Rh^{103}(p,4n)Pd^{100}$ reaction ($Q=-28.2$ MeV).[7] After dissolution of the rhodium target, palladium was extracted carrier-free into chloroform as the dimethylglyoxime complex.

† Work supported by the U. S. Atomic Energy Commission.
* National Science Foundation Fellow.
[1] L. Marquez, Phys. Rev. **92**, 1511 (1953).
[2] Chart of the Nuclides (Knolls Atomic Power Laboratory), 6th and 7th eds. In a private communication, Dr. D. T. Goldman, editor of this chart, reports that his correspondence files do not reveal the author of this otherwise unreported work.
[3] M. Koike, K. Hisatake, N. Ono, and K. Takahashi, Nucl. Phys. **54**, 129 (1964).
[4] J. S. Evans, E. Kashy, R. A. Naumann, and R. F. Petry, Phys. Rev. **138**, B9 (1965).
[5] I. M. Rogachev and M. K. Nikitin, Izv. Akad. Nauk. SSSR, Ser. Fiz. **28**, 72 (1964).
[6] N. M. Anton'eva, M. K. Nikitin, and V. B. Smirnov, Zh. Eksperim. i Teor. Fiz. **46**, 1490 (1964) [English transl.: Soviet Phys.—JETP **19**, 1008 (1964)].
[7] V. A. Kravtsov, Nucl. Phys. **41**, 330 (1963).

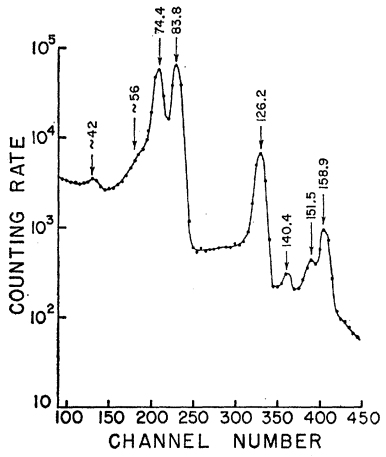

FIG. 1. Gamma-ray spectrum of a Pd^{100} source. The energies are average values from two similar spectra. Only a few of the data points have been plotted for clarity.

Sources for gamma-ray studies consisted of portions of the chloroform extract in sealed plastic containers. For conversion-electron spectroscopy, palladium was electroplated carrier-free from an aqueous buffer solution onto platinum source backings. Further details of the radiochemical procedures have been reported elsewhere.[4] The Pd^{100} sources contained Pd^{103} (17 days) and usually also Pd^{101} (8.4 h).

III. GAMMA-RAY SPECTRUM

A lithium-drifted germanium detector[8] was used to obtain the gamma-ray spectrum of Pd^{100} shown in Fig. 1. The single transition reported by Marquez was shown to be a prominent doublet, and several additional peaks between 100 and 160 keV were found. All gamma rays from Pd^{100} sources, above 200 keV, were identified as arising from the decay of the Rh^{100} daughter. Energies and relative intensities for the gamma rays assigned to Pd^{100} decay are listed in Table I. The energies were obtained by linear interpolation from calibration spectra using Hg^{203}, Na^{22}, Cs^{137}, and Au^{195} sources. The line shape of the well-resolved 126-keV photopeak was used to decompose the composite photopeaks into their constituents. No adjustment of the width of the line shape was necessary in this energy range. The height of each peak was divided by the germanium photoelectric cross section,[9] to yield the relative intensity. The intensities in Table I are average values, obtained by analyzing spectra from two separate bombardments. The two values agreed within 5% for the three prominent lines, but differed by as much as 35% for the weaker lines.

TABLE I. Gamma rays from Pd^{100} decay.

Energy (keV)[a]	Relative intensity[b]
<60	<1.5
74.4	69.8
83.8	100.0
126.2	33.4
140.4	1.2
151.5	2.5
158.9	8.2

[a] The error is estimated, from the nonlinearity of calibration spectra and the agreement of several spectra, to be about 0.5 keV.
[b] Normalized to the most intense line.

IV. CONVERSION-ELECTRON SPECTRA

High-resolution conversion-line spectra were photographically recorded with two permanent-magnet spectrographs, covering the energy ranges 5 to 130 and 10 to 440 keV. A typical spectrum, showing the major transitions, is shown in Fig. 2. Conversion-electron energies, averaged from a large number of spectrographic plates, are given in Table II. Previously reported conversion-electron energies are given for comparison in Table II. Using the precise energies from Table II and the atomic binding energies tabulated by Hill *et al.*,[10] transition energies were calculated. In averaging, each K line was given a relative weight of 10 per observation, each L line a weight of 5 per observation, and each M line a weight of one per observation. The transition energies calculated in this way are presented in Table III.

Conversion-electron spectra were also obtained with a six-gap beta-ray spectrometer (the "orange" spectrometer design of Kofoed-Hansen *et al.*[11]). These spectra were similar to that reported by Anton'eva *et al.*[6] In order to determine absolute conversion coefficients for the 75- and 84-keV transitions, both Pd^{100} and Cs^{137} sources were measured in the orange spectrometer under

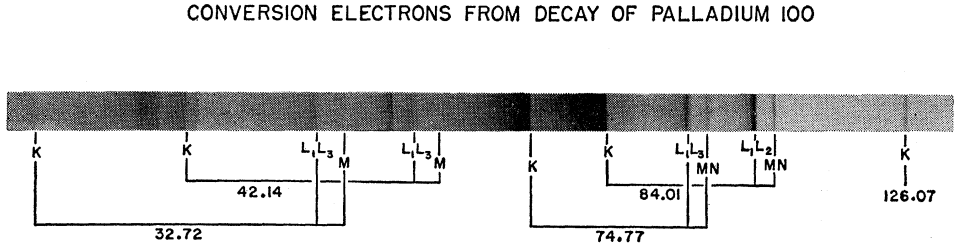

FIG. 2. Spectrographic plate showing conversion electrons from the major transitions in Rh^{100}. Also visible are Auger electrons (near the $K42$ line) and L conversion electrons of a 40-keV isomeric transition in Rh^{103} (to the left of $L42$ lines).

[8] Purchased from RCA Victor, Ltd., Montreal, Canada.
[9] Interpolated from the theoretical values of C. M. Davisson and R. D. Evans, Rev. Mod. Phys. **24**, 79 (1952).
[10] R. D. Hill, E. L. Church, and J. W. Mihelich, Rev. Sci. Instr. **23**, 523 (1952).
[11] O. Kofoed-Hansen, J. Lindhard, and O. B. Nielsen, Kgl. Danske Videnskab. Selskab, Mat. Fys. Medd. **25**, No. 16 (1950); O. B. Nielsen and O. Kofoed-Hansen, *ibid.* **29**, No. 6 (1955).

identical conditions and also with a NaI gamma-ray detector. The partition of the composite (75+84)-keV Pd^{100} photopeak was accomplished using the intensity ratio of the 75- and 84-keV photons from Table I. The experimental K conversion coefficient for the 662-keV transition in Ba^{137} is reported to be 0.093.[12] The relative electron and gamma intensities are given in Table IV, together with the experimental and theoretical conversion coefficients. It is concluded that the 75-keV transition is $E1$, perhaps with an anomalous conversion coefficient. The 84-keV transition is predominantly $M1$, since a large $E2$ admixture would have made the L_{II} and L_{III} lines more prominent on the photographic plates than is actually observed. From approximate L subshell intensities on the photographic plates, and from relative conversion-electron intensities and $K/L/M$ ratios in orange spectrometer spectra, the probable multipolarities of the remaining transitions have been deduced as shown in Table III. Numerical values for conversion coefficients are not given, because the variation of detection efficiency in the spectrometer is not known in this energy range.

TABLE II. Conversion electrons from Pd^{100} sources.

Conversion-electron energy (keV)				
Present work[a]	Koike *et al.*[b]	Rogachev and Nikitin[c]	Anton'eva *et al.*[d]	Assignment
9.52±0.04		9.02±0.19	9.2±0.2	K
16.57±0.08		16.47±0.20		K[e]
18.89±0.04			18.6±0.5	K
29.29±0.06		29.01±0.30	29.0±0.2	L_I
29.57±0.13[f]				L_{II}
29.70±0.07				L_{III}
32.12±0.08			31.8±0.2	M_I
32.61±0.14[f]		32.50±0.30	28.5±0.5	K
36.66±0.04		36.15±0.20		L_{II}[e]
36.82±0.04				L_{III}[e]
38.71±0.07				L_I
39.25±0.08		38.37±0.20		M_I[e]
41.47±0.08				M_I
51.57±0.07	46.2±0.3	51.16±0.17	51.2±0.4	K
60.79±0.08	55.6±0.3	60.57±0.36	60.6±0.4	K
71.35±0.08	67.5±0.4	71.10±0.35	71.2±0.4	L_I
71.62±0.18[f]				L_{II}
71.76±0.18[f]				L_{III}
74.14±0.10			74.0±0.4	M_I
80.59±0.08	78.0±0.4	80.30±0.35	80.5±0.5	L_I
80.89±0.16[f]				L_{II}
83.35±0.11			83.4±0.4	M_I
102.88±0.20	100 ±1		103.3±0.5	K
116.51±0.19[f]				K
122.51±0.30[f]				K
128.34±0.30[f]				K
135.56±0.34			134.9±0.5	K

[a] The tabulated error in each case is the standard deviation based on several measurements, typically about 15.
[b] The lines reported in Ref. 3 have been assigned by the present authors.
[c] Reference 5.
[d] Reference 6.
[e] Assigned to the 39.80-keV isomeric transition in Rh^{103}.
[f] This line was observed very infrequently on photographic plates; the quoted error is an estimate.

TABLE III. Transitions in Rh^{100}.

Energy (keV)[a]	Multipolarity	Relative intensity[b]
32.72±0.06	$M1+E2$	87[c]
42.10±0.05	$E1$	51
55.82±0.14	$M1$[d]	3.4
74.77±0.08	$E1$	94
84.00±0.09	$M1$	159
126.07±0.19	$E1$	36
139.72±0.30	$M1$[d]	1.4
151.55±0.30	$E1$[d]	2.8
158.77±0.34	$E1$	8.5

[a] The errors are standard deviations computed using all observations of each transition.
[b] Transition intensities were computed from gamma-ray intensities using theoretical conversion coefficients for the assigned multipolarity. The units are the same arbitrary units as in Table I.
[c] Minimum amount required for consistency with proposed decay scheme.
[d] Deduced from gamma intensity and parity considerations.

V. COINCIDENCE STUDIES

The orange spectrometer was used to detect conversion electrons, and 3-in.×3-in. NaI scintillation crystals were employed to detect photons. A standard Chase coincidence circuit was used in all of the coincidence experiments.

A. Conversion-Electron–Gamma Coincidences

Gamma-ray spectra were observed in coincidence with L conversion electrons of the 33-keV transition and with K conversion electrons of the 75- and 84-keV transitions. Both prompt and random coincidences were recorded simultaneously in separate halves of a multichannel analyzer by means of routing pulses from the coincidence circuit. The net coincidence spectra are shown, together with a singles spectrum, in Fig. 3. These spectra confirm the 126–33-, 84–42–33-, and 84–75-keV cascade sequences reported by Anton'eva *et al.*[6] In addition, there is a 56-keV photon in coincidence with the 33-, 75-, and 84-keV transitions. The peak at 65 keV in Figs. 3(b) and (c) is attributed to a platinum x ray (66.3 keV), following a photoelectric interaction of an 84-keV photon with the platinum source backing. This conclusion is justified by the absence of this 65-

TABLE IV. Conversion coefficients for transitions in Rh^{100}.

	Cs^{137}	Pd^{100}	Pd^{100}
Photon energy (keV)	662	75	84
K conversion-electron intensity	100.0	23.7	43.4
Photon intensity[a]	100.0	5.20	7.44
K conversion coefficient	0.093[b]	0.42	0.54
Theoretical K conversion coefficient[c]: $E1$		0.300	0.215
$M1$		0.710	0.505
$E2$		2.88	1.94

[a] Corrected for photopeak efficiency.
[b] Reference 12.
[c] Reference 13.

[12] *Nuclear Data Sheets*, compiled by K. Way *et al.* (Printing and Publishing Office, National Academy of Sciences—National Research Council, Washington 25, D. C., 1961), NRC 61-1-63 through 61-1-71, 61-2-32, 61-2-134.

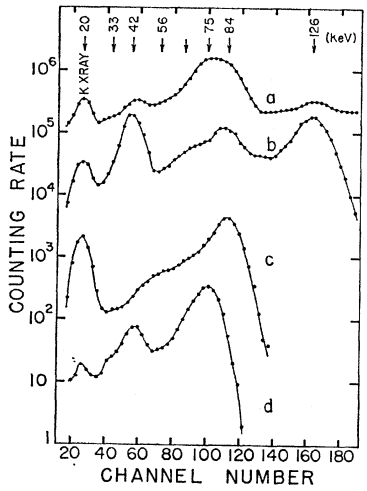

FIG. 3. Conversion electron-gamma coincidence spectra: (a) singles spectrum; (b) spectrum gated by L conversion electrons of 33-keV transition; (c) spectrum gated by K conversion electrons of 75-keV transition; (d) spectrum gated by K conversion electrons of 84-keV transition. The shoulder at channel 86 in (b) and (c) is assigned to a Pt x ray (see text).

keV peak when K conversion lines of the 84-keV transition provided the coincidence gate [see Fig. 3(d)], since the 75-keV photons do not have sufficient energy to eject a K photoelectron from platinum (K binding energy, 78.4 keV). The photon intensity ratios in these coincidence spectra have been used to establish gamma-ray intensities for the low-energy photons which were not directly observable with the lithium-drifted germanium detector. The gamma-ray intensities and theoretical conversion coefficients[13] yielded the transition intensities which are given in Table III.

B. Lifetime of the 75-keV Level

The prominent 75–84-keV cascade exhibited a delayed-coincidence curve when the counting rate was measured as a function of artificial delay imposed in one circuit. It is possible to determine which transition is delayed in such a cascade if the two transition energies can be distinguished, since the delayed-coincidence curve is then asymmetric. The half-life of the intermediate state can be computed from the slope of the delayed-coincidence curve.[14] In a typical run, shown in Fig. 4, the K conversion electrons of the 84-keV transition were focused in the orange spectrometer for one channel, and the composite (75+84)-keV photopeak from a scintillation detector was selected with a discriminator window for the second channel. The coincidence counting rate was obtained at several values of artificial delay in the electron channel. The delay was introduced electronically at the coincidence circuit, which had been calibrated with an oscilloscope. A resolving time of approximately 0.1 μsec was used.

As seen in Fig. 4, some 75-keV photons were detected even when the electron gate was delayed nearly one microsecond. The converse coincidence experiment was also performed, using K conversion electrons of the 75-keV transition and 84-keV photons. As expected, electrons corresponding to the 75-keV transition were detected in coincidence, even when the photon gate was delayed up to one microsecond. In each case when the relative delay was reversed, the coincidence counting rate dropped sharply to the expected chance rate. These experiments conclusively demonstrate that the 75-keV transition *follows* the 84-keV transition. A mean value of 0.18 ± 0.02 μsec was computed from the slope of the delayed-coincidence curves for the lifetime of the nuclear state which deexcites by means of the 75-keV transition. It will be shown subsequently that this state is in fact located 75 keV above the Rh^{100} ground state.

C. Anisotropy of the 84–75-keV Cascade

The anisotropy of the 84–75-keV cascade was measured in order to place limits on the spins of three levels in Rh^{100}. The anisotropy A is defined by the expression

$$A=[W(180°)-W(90°)]/W(90°)\,, \qquad (1)$$

where $W(\theta)$ is the coincidence counting rate when the two detectors make an angle θ with the source. Two 3-in.×3-in. NaI detectors were placed about 10 in. from the source. Energy discrimination in each channel passed only the (75+84)-keV photopeak to the coincidence circuit, which operated at a resolving time of approximately 0.1 μsec. The coincidence counting rates at 180 and 90° were normalized to the geometric mean of the two singles rates, in order to correct for source decay and electronic drifts. The number of random events cancels out in the numerator of (1) but not in the denominator. Although the maximum delay available (0.75 μsec) was not sufficient to reach the random-coincidence rate with certainty (owing to the delayed-coincidence effect), nevertheless, the difference between the random rate obtained and that expected (computed

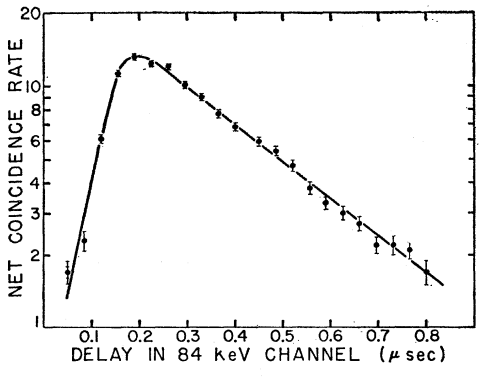

FIG. 4. Delayed-coincidence curve for the 84–75-keV cascade. The abscissa is artificial electronic delay in the signal from K conversion electrons of the 84-keV transition relative to the undelayed signal from 75-keV photons. The choice of zero delay is completely arbitrary and does not necessarily correspond to a prompt coincidence event. Purely random events (obtained experimentally at "negative" delay) have been subtracted.

[13] M. E. Rose, *Internal Conversion Coefficients* (North-Holland Publishing Company, Amsterdam, 1958).

[14] R. E. Bell, *Beta- and Gamma-Ray Spectroscopy*, edited by K. Siegbahn (North-Holland Publishing Company, Amsterdam, 1955), Chap. XVIII.

from the resolving time and singles rates) represented a smaller error in the denominator of (1) than the purely statistical uncertainty in the numerator. The result obtained was $A=+0.17\pm0.03$, where the error is computed solely from the counting statistics. After a small correction was applied for the finite solid angle of the detectors, the experimental anisotropy was found to be $A=+0.18\pm0.03$.

VI. Rh^{100} LEVEL SCHEME

The level scheme for Rh^{100} suggested by Anton'eva *et al.*[6] is shown in Fig. 5(a); an inverted scheme accommodating the same transitions is shown in Fig. 5(b). Both schemes (a) and (b) are fully consistent with the coincidence spectra (see Fig. 3). Furthermore, the two alternatives would not be distinguishable by a detailed transition-intensity balance, if electron-capture feeding should happen to occur only at the 159-keV level in (a) and (b). The choice of scheme (b) is demanded by the establishment of delayed coincidences in the 84–75-keV cascade. Scheme (b) allows the 75-keV transition to be delayed following an 84-keV transition, in accord with the experimental results; the converse is required by scheme (a). Although the delayed-coincidence experiment would allow some other transition to follow the 75-keV transition in (b), the 56-keV transition observed in coincidence has insufficient intensity to permit locating it below the 75-keV transition.

The four major levels in Fig. 5(b) are connected by all six possible transitions, and the transition energy sums and differences check within an average precision of 0.03 keV. Since there is no evidence for any other strong transition with energy greater than 10 keV, the four levels in Fig. 5(b) appear to be established unambiguously, with the level labeled 0 actually the Rh^{100} ground state and with excited states occurring at 32.70, 74.79, and 158.77 keV. The required coincidences between the transitions have been observed: 33–42, 33–84, 33–126, 75–84, and 84–42 keV. Since the coincidence data indicates that the 56-keV transition is in coincidence with the 33-, 75-, and 84-keV transitions, it is placed between a new level at 214.6 keV and the

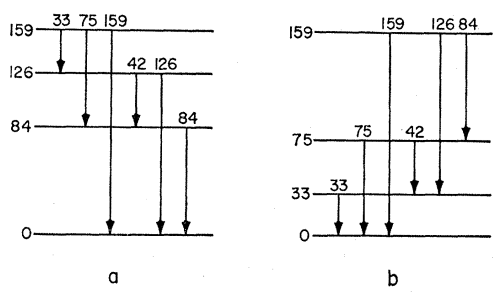

FIG. 5. Two possible partial level schemes for Rh^{100}: (a) scheme proposed in Ref. 6; (b) scheme deduced from this investigation. The two schemes accommodate the same transitions and implied coincidences.

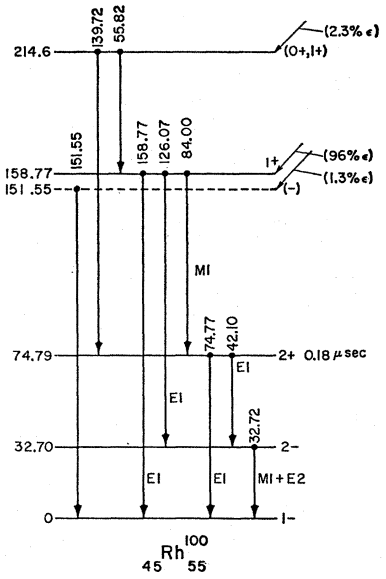

FIG. 6. Level scheme for Rh^{100} as deduced from Pd^{100} decay data. The multipolarities shown are felt to be definitely established. The level at 214.6 keV is not conclusively established, and the 151.55-keV level is strictly conjectural (see text). The spins which are not enclosed within parentheses form a mutually consistent set which is thought to be uniquely consistent with the data.

158.77-keV level. The new level will then accommodate the very weak 140-keV line, although no confirmation of this latter placement was found in the coincidence experiments. The complete level scheme proposed for Rh^{100} is given in Fig. 6.

Spins and parities of the levels may be deduced with considerable certainty from the data. The absence of evidence for population of levels higher than 215 keV in the decay of Pd^{100} points to a modest decay energy, i.e., <500 keV, and this fact, coupled with the 4-day Pd^{100} half-life, dictates allowed decay for the major feed at the 158.77-keV level. Since the 158.77-keV level must be 0+ or 1+, the predominantly $M1$ character of the 84-keV transition requires positive parity and spin 0, 1, or 2 for the 74.79-keV level. It is difficult to obtain the conversion electron intensity, multipolarity mixture, and transition intensity of the 33-keV transition precisely, because the detection efficiency of the orange spectrometer is not known in this energy range. Nevertheless, the available data would be very inconsistent with an allowed decay branch to the 74.79-keV level. This situation forces the adoption of spins 2+ and 1+ for the 74.79- and 158.77-keV levels, respectively.

The $E1$ character of the 75-keV transition and the $M1+E2$ character of the 33-keV transition establish negative parity for the 0- and 32.70-keV levels. These two levels must then each have spin and parity 1− or 2− in order to allow the 42-, 126-, and 159-keV transitions to have $E1$ multipolarity. The photon intensity of these transitions is too large to permit an appreciable admixture of $M2$ multipolarity. The assumption that the 0- and 32.70-keV levels are 1− and 2− or 2− and 1−, respectively, is reasonable, since the existence of two levels only 33 keV apart with the same $I\pi$ appears unlikely. The established spins of the 74.79 (2+) and 158.77 (1+) keV levels, the observed predominant $M1$

and $E1$ character of the 84- and 75-keV transitions, and the alternate choices 1− or 2− for the ground state of Rh^{100} indicate the spin sequences $1(1)2(1)J$ for the 84–75-keV cascade, where $J=1$ or 2. The theoretical anisotropies[15] for these sequences are $A(J=1)=+0.288$ and $A(J=2)=-0.241$. The positive experimental anisotropy $A_{\text{exp}}=+0.18\pm0.03$ then establishes the ground state of Rh^{100} as 1−.

The Nuclear Data Group[12] has interpreted the data of Marquez[1] for the positron decay of Rh^{100} in terms of a 2− spin for Rh^{100}, although Marquez was unable to demonstrate a unique shape for the positron branch to the ground state of Ru^{100} ($\log ft=8.6$). The lower $\log ft$ value of 8.1 reported by Koike *et al.*[3] was calculated by assuming, *a priori*, unique first-forbidden decay from a 2− Rh^{100} ground state to the 0+ Ru^{100} ground state. Unless the shape of the Rh^{100} positron spectrum can be measured precisely, the gamma-ray anisotropy data is probably the most conclusive evidence available at this time for establishing the ground state of Rh^{100} as 1−. The 32.70-keV level is then most probably a 2− state, although 1− is a formal but unlikely possibility.

These spin assignments and the theoretical conversion coefficients[13] permit a transformation of the gamma-ray intensities in Table I into the transition intensities in Table III. By analogy with the high relative intensity of the $M1$ transition (84 keV) depopulating the 158.77-keV level compared to the $E1$ transitions (126 and 159 keV), the 56- and 140-keV transitions are assumed to be $M1$. The 214.6-keV level then has $I\pi=0+$ or 1+, and the possible $E1$ transitions to the 32.70- and 0-keV levels are presumed to be too weak to be observed. The weak 152-keV transition cannot be located by energy sum relationships or by the coincidence data. In order to accommodate this weak transition, a 151.55-keV level with negative parity is tentatively proposed.

The transition intensities in Table III do not provide sufficient evidence to determine $\log ft$ values. If the Pd^{100}-Rh^{100} mass difference is assumed to be 400 keV, then decay to the 158.77-keV level has $\log ft=4.6$, and the branch to the 214.6-keV level has $\log ft=5.9$. Since the evidence suggests allowed decay to both the 214.6- and 158.77-keV levels, the Pd^{100}-Rh^{100} mass difference probably lies in the range 350 to 425 keV, unless one or both $\log ft$ values are anomalous. Within this range of total decay energy, the $\log ft$ for decay to the 151.55-keV level would be about 6.5.

VII. DISCUSSION

The measured lifetime of $(1.8\pm0.2)\times10^{-7}$ sec for the 74.79-keV level may be combined with the gamma-ray and total transition intensities of the 75- and 42-keV $E1$ transitions (see Tables I and III) to give a radiative lifetime of 3.7×10^{-7} sec for the 75-keV transition. This value may be compared with the Weisskopf theoretical estimate of 7.5×10^{-13} sec for such an $E1$ transition, indicating a retardation factor of 5×10^5. The ratio of the observed gamma-ray intensities of the 75- and 42-keV transitions is 3.7, while the corresponding ratio of the Weisskopf theoretical transition probabilities is 5.6. It is then apparent that the two $E1$ transitions depopulating the 74.79-keV level are each hindered by about the same amount, namely, a factor of 4×10^5. Using the Weisskopf estimates, one computes that the 126- and 159-keV $E1$ gamma rays are hindered by factors of 700 and 6000, relative to the 84-keV $M1$ gamma ray. But since pure $M1$ transitions are often slower by a factor of 10 to 1000 than the Weisskopf estimate,[16] it appears that every $E1$ transition observed in Rh^{100} is retarded by a factor of about 10^5.

The large inhibition in $E1$ gamma-ray emission suggests a substantial difference in nuclear structure between the positive- and negative-parity levels in Rh^{100}. In this mass region, only positive-parity states are known at low energies in nuclei with even Z and odd N. In nuclei with odd Z and even N, on the other hand, it is common to find closely competitive $(g_{9/2})^n$ and $(g_{9/2})^{n-1}p_{1/2}$ proton configurations, giving rise to $\frac{9}{2}+$, $\frac{7}{2}+$, and $\frac{1}{2}-$ states.[4] As expected, numerous $E3$ and $M4$ isomeric transitions are known. It is reasonable to postulate that the $(g_{9/2})^5$ and $(g_{9/2})^4p_{1/2}$ proton configurations make the predominant contributions to the positive- and negative-parity states in Rh^{100}, respectively. Under this assumption, the transitions between positive- and negative-parity states in Rh^{100} would then involve a $\Delta l=3$ orbital-angular-momentum change for the protons. The $E1$ transitions are probably accomplished via small admixtures of other configurations.

The principal neutron configuration contributing to the ground states of odd-N, even-Z nuclides in this mass region is probably $(d_{5/2})^n$, as suggested by the ground-state spins $\frac{5}{2}$.[12] Similarly, the low-lying $\frac{1}{2}+$ states and the ground-state spin $\frac{1}{2}+$ of Mo^{99} ($N=57$) and Mo^{101} ($N=59$) indicate that the location of the $s_{1/2}$ single-particle shell-model state[17] lies above the $d_{5/2}$ state. A $\frac{3}{2}+$ first excited state has been located in Ru^{99} ($N=55$) at 90 keV, which decays to the $\frac{5}{2}+$ ground state via a mixed $M1+E2$ transition $[(E2/M1)=2.4\pm0.9]$. Since the $E2$ portion shows enhancement by a factor of 50 over the single-particle rate,[18] this state has considerable collective character. A $\frac{3}{2}+$ first excited state lying at 127 keV has been found[12] in Ru^{101}($N=57$), which we presume is similar to the first excited state of Ru^{99}.

The jj-coupling rules proposed by Brennan and Bernstein[19] have been very successful in predicting spins

[15] H. Frauenfelder, *Beta- and Gamma-Ray Spectroscopy*, edited by K. Siegbahn (North-Holland Publishing Company, Amsterdam, 1955), Chap. XIX.

[16] A. H. Wapstra, G. J. Nijgh, and R. Van Lieshout, *Nuclear Spectroscopy Tables* (North-Holland Publishing Company, Amsterdam, 1959).

[17] S. A. Hjorth and B. L. Cohen, Phys. Rev. **135**, B920 (1964).

[18] O. C. Kistner, S. Monaro, and A. Schwarzschild, Phys. Rev. **137**, B23 (1965).

[19] M. H. Brennan and A. M. Bernstein, Phys. Rev. **120**, 927 (1960).

and magnetic moments for low-lying levels in odd-odd nuclei. According to rule $R2$ of that coupling model, a ground state with spin given by $|J_P \pm J_N|$ is expected from the coupling of J_P and J_N, the resultant spins of the proposed proton and neutron configurations. Actually, Brennan and Bernstein restricted the application of their rules primarily to ground states, together with a few excited states whose spins were well established experimentally. It is interesting to inquire to what extent the states of Rh^{100}, found in these studies, can be interpreted by an extension of this model.

The negative parity of the ground state and first excited state of Rh^{100} can easily be understood by invoking the proton configuration $[(g_{9/2})^4 p_{1/2}]_{\frac{1}{2}}$, which is known for the ground state of odd-A Rh isotopes.[4] To account for the Rh^{100} 1− ground state using the Brennan-Bernstein coupling rules, one must additionally employ a positive-parity neutron configuration coupled to spin $J_N=\frac{1}{2}$ or $\frac{3}{2}$. Similarly the 2− excited state may be accounted for, using $J_N=\frac{3}{2}$ or $\frac{5}{2}$. The $J_N=\frac{3}{2}$ choice is attractive, in that its employment accounts for both of the negative-parity states. However, it should be noted that the collective character of the known $\frac{3}{2}+$ first excited state in Ru^{99} casts considerable doubt on participation of an analogous $\frac{3}{2}+$ state in Rh^{100} levels, which we presume to be formed from single-particle configurations. Since the character of the other excited states in odd-A Ru isotopes, particularly Ru^{99}, has not yet been established, a preference cannot yet be indicated for the likely neutron single-particle configurations for $N=55$. Accordingly, we indicate the neutron configurations for Rh^{100} states by the general notation $[(d_{5/2})^{5-n}(s_{1/2})^n]J_N$, where $J_N=\frac{1}{2}, \frac{3}{2}, \frac{5}{2}$ and $0<n<2$. The proposed proton and neutron configurations for each Rh^{100} level are given in Table V.

Perhaps it is interesting to note that certain other spins, namely, 0−, 3−, 6+, and 7+ are also predicted to arise from the same configurations using rule $R2$. In the cases treated by Brennan and Bernstein, the two states with spins $|J_P+J_N|$ and $|J_P-J_N|$ often occurred very close together. Although there is no evidence for their existence from the present work, there is the possibility that high-spin levels (3−, 6+, or 7+) exist in Rh^{100} below 400 keV. Isomers have been found or suggested in Rh^{102}, Rh^{104}, and Rh^{106}, as well as in odd-odd Tc and Ag nuclei.[12] No isomeric behavior has been reported for Rh^{100} samples prepared by (p,n) reactions on Ru^{100} at[20] 6.7 and 13 MeV.[3]

TABLE V. Proposed configurations of the levels in Rh^{100}.

Proton configuration	Neutron configuration	Spin and parity	Observed energy (keV)
$[(g_{9/2})^4 p_{1/2}]_{\frac{1}{2}}$	$[(d_{5/2})^{5-n}(s_{1/2})^n]_{\frac{1}{2}}$ or $\frac{3}{2}$	1−	0
$[(g_{9/2})^4 p_{1/2}]_{\frac{1}{2}}$	$[(d_{5/2})^{5-n}(s_{1/2})^n]_{\frac{3}{2}}$ or $\frac{5}{2}$	2−	32.70
$(g_{9/2})^5{}_{\frac{9}{2}}$	$[(d_{5/2})^{5-n}(s_{1/2})^n]_{\frac{5}{2}}$	2+	74.79
$(g_{9/2})^5{}_{\frac{7}{2}}$	$[(d_{5/2})^{5-n}(s_{1/2})^n]_{\frac{3}{2}}$		
$(g_{9/2})^5{}_{\frac{7}{2}}$	$[(d_{5/2})^{5-n}(s_{1/2})^n]_{\frac{5}{2}}$	1+	158.77

Brennan and Bernstein have suggested that further testing of the validity of their coupling rules would be desirable. None of the original examples included predictions for more than two excited states in any single nucleus, because spins were not experimentally determined for very many excited states. Perhaps Rh^{100} is the most neutron-deficient nucleus to which the Brennan-Bernstein rules have thus far been applied. Although no spins have been measured directly, it has been shown that the spins of four levels in Rh^{100} seem uniquely determined by beta- and gamma-transition selection rules. Furthermore, it is gratifying that the ordering of these levels (see Table V and Fig. 6) is consistent with the level ordering $\frac{1}{2}-<\frac{9}{2}+<\frac{7}{2}+$ recently found[4] for the levels in Rh^{101}, which are attributable to the same proton configurations as proposed here. It would be interesting to obtain further information concerning the nature of the low-lying levels in the $N=55$ isotones Mo^{97}, Ru^{99}, and Pd^{101}.

ACKNOWLEDGMENTS

We wish to thank Dr. W. Goodell and the staff of the Nevis Synchrocyclotron, Columbia University, for arranging and performing the irradiations of our rhodium targets. We appreciate the stimulating discussions we have had with Professor B. Bayman and Professor J. D. McCullen, and we are grateful for their helpful comments and suggestions.

[20] J. P. Blaser, F. Boehm, P. Marmier, and P. Scherrer, Helv. Phys. Acta 24, 441 (1951).

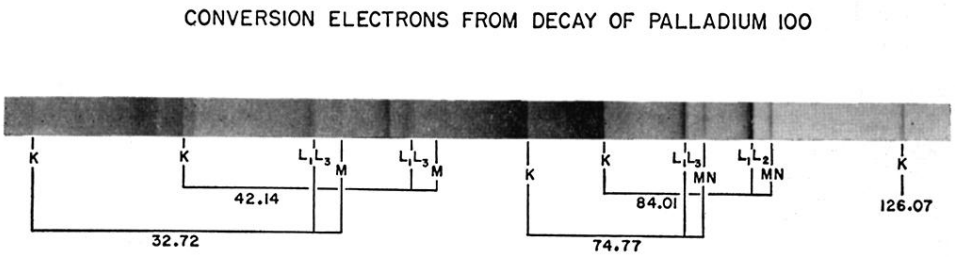

FIG. 2. Spectrographic plate showing conversion electrons from the major transitions in Rh^{100}. Also visible are Auger electrons (near the $K42$ line) and L conversion electrons of a 40-keV isomeric transition in Rh^{103} (to the left of $L42$ lines).